Journal of the Turkish Chemical Society
Section: B
Chemical Engineering
Turkish Chemical Society

RSM Optimization of Direct Orange 26 Adsorption on Low-Cost Silica Fume Adsorbent

Shohre Mortazavi*, Ebrahim Najafi Kani

[1]Semnan University, Department of Chemical, Petroleum, and Gas Engineering, Semnan, Iran

Abstract: Today, dye pollutants enter resources of water through various industries. Due to the stability and carcinogenicity of dye pollutants, it is necessary to treat colored wastewater before entering the aqueous cycle. One of the important methods for wastewater treatment is adsorption. In this study, the effect of industrial waste of silica fume adsorbent on azo dye Direct Orange 26 (DO26) was investigated. Design of experiment was carried out with CCD method by using Design Expert software version 7 to model and investigate the effects of parameters pH, concentration, amount of adsorbent, and time. The model proposed by the software is a second-order model. According to the findings, important and effective parameters for the quadratic model of experimental design were obtained from ANOVA (analysis of variance). The optimum conditions for the maximum removal of DO26 (95.26%) were obtained to be at pH 2.01, contact time of 55.15 minutes, adsorbent amount of 0.2 g, and initial concentration of 44 ppm. The experimental kinetic data were analyzed through the conventional kinetic models, and the results demonstrate that the sorption kinetics can be accurately described by the pseudo-second order model. Also, based on FESEM image, silica fume has a spherical and porous structure, therefore, silica fume can remove dye pollutants from water as a cheap adsorbent.

Keywords: Response surface method, wastewater, adsorption, silica fume.

Submitted: January 23, 2023. **Accepted:** July 05, 2023.

Cite this: Mortazavi, S., & Najafi Kani, E. (2023). RSM Optimization of Direct Orange 26 Adsorption on Low-Cost Silica Fume Adsorbent. *Journal of the Turkish Chemical Society, Section B: Chemical Engineering*, *6*(2), 35–44. **DOI:** https://doi.org/10.58692/jotcsb.1240859

*Corresponding author. E-mail: mortazavi@semnan.ac.ir.

1. INTRODUCTION

Today, industrial pollutants enter resources of water and shortage of water is a serious crisis (Yan et al., 2015). Dyes and pigments enter water through industries such as plastic, food, cosmetics, printing, etc. (Genc & Oguz, 2010). Synthetic dyes have a complex aromatic molecular structure, therefore, it is difficult to remove dye pollutants from water (Sohrabi et al., 2016). Also, toxic and carcinogenic nature of dyes threatens health of humans (Kannaujiya et al., 2022). Long-term contact with these dyes causes disorders such as nausea, bleeding, wounds on the skin, and serious damage to vital organs. Therefore, correct and effective treatment of dye pollutants before entering water cycle is necessary (Ghaedi et al., 2015; Zhu, Zhang, & Yan, 2016).

Direct Orange 26 (DO26) is used in coloring cellulosic fibers such as yarn, linen, synthetic silk, as well as in coloring leather and paper (Safa & Bhatti, 2011). This dye causes harmful effects in case of contact with eyes and skin (Aşçı, 2013). One of the effective methods for removing textile dyes from wastewater is adsorption (Geyikçi et al., 2012). Safa et al. (2011) investigated removal of DO26 dyes from aqueous solutions by rice husk (Safa & Bhatti, 2011). Tomczak et al. (2014) investigated sorption of DO26 onto a cheap plant sorbent (Tomczak & Tosik, 2014).

Silica fume, which is also known as microsilica, is a gray powdery solid with pozzolanic properties containing amorphous silica. In the past, the dust obtained from ferrosilicon arc furnaces was considered as waste of this process (Li et al., 2014). Today, with the advancement of technology and attention to the optimal use of industrial waste, this dust is marketed as a by-product under the brand name of silica fume. Due to the unique properties of silica fume, including high porosity and permeability, very small particle size, low specific gravity, high specific surface area, low thermal conductivity, good absorption capacity, and chemical inertness, it has received special attention (Zhang et al., 2012). The unique properties of silica fume have led to its use in the cement industry, the production of polymer products, and the absorption of pollutants (Ahmed, Gaber, & Rahim, 2017). Wang et al. (2011) found that the performance of silica fume in adsorption of Rhodamine B from aqueous solutions is better than from coal ash (Wang & Chu, 2011). Kalkan et al. (2014) found silica fume has a high capacity to adsorb nickel (Kalkan, Nadaroglu, & Celebi, 2014). Nadaroglu et al. (2013) and Ahmed et al. (2015) showed that silica fume is a cheap and effective adsorbent for the removal of cadmium (II) and copper and zinc ions from wastewater (Ahmed et al., 2017; Nadaroglu & Kalkan, 2014).

Experiment design causes process evaluation, process efficiency improvement, design selection in such a way that the product or output works well in different conditions, determination of key process parameters that have the greatest impact on process output (Montgomery, 2017). Due to the low cost and high porosity of silica fume, in this study, RSM optimization of DO26 adsorption on low-cost adsorbent silica fume from wastewater has been investigated.

2. EXPERIMENTAL SECTION

2.1 Materials and Methods

Direct Orange 26 (DO26), with the experimental formula $C_{33}H_{22}N_6Na_2O_9S_2$ is an azo dye used in the dyeing of cellulose fibers, leather, and paper (Safa & Bhatti, 2011). The molecular weight of DO26 is 756.67, the solubility in water is 50 g/L, and the maximum absorption wavelength is 495 nm.

Silica fume was obtained from Lorestan Ferroalloy Company without any operations. To prepare the adsorbent, silica fume was passed through a 60-mesh sieve. Then the adsorbent was kept in plastic containers to prevent its contact with pollution and moisture. The specific surface area of silica fume is 18.0 m^2/g. Chemical composition and surficial properties of silica fume (determined by X-ray fluorescence) are shown in Table 1. In addition, the maximum wavelength of the used colors was measured by the UV-spectrophotometer (PC 1650-UV, Shimadzu, Japan), and pH meter model AZ8686 with accuracy of ± 0.01 for pH adjustment used in the adsorption process. Materials were weighed by a digital scale (GK-1203, Sartorius, Germany) and a hot plate magnetic stirrer (TA-105, VELP, France) is used to mix the materials in experiments. Field Emission Scanner Electronic Microscopy (FESEM, JSM 6400, JEOL, Japan) is used to identify the microstructure of the adsorbent. Figure (1) shows FESEM image of silica fume.

Table 1. Chemical composition and surficial properties of silica fume.

SiO_2 (wt. %)	Al_2O_3 (wt. %)	K_2O (wt. %)	Density (kg/m^3)	Specific Surface (m^2/g)	Pore Diameter µm
96.12	0.82	0.4	213	18	13

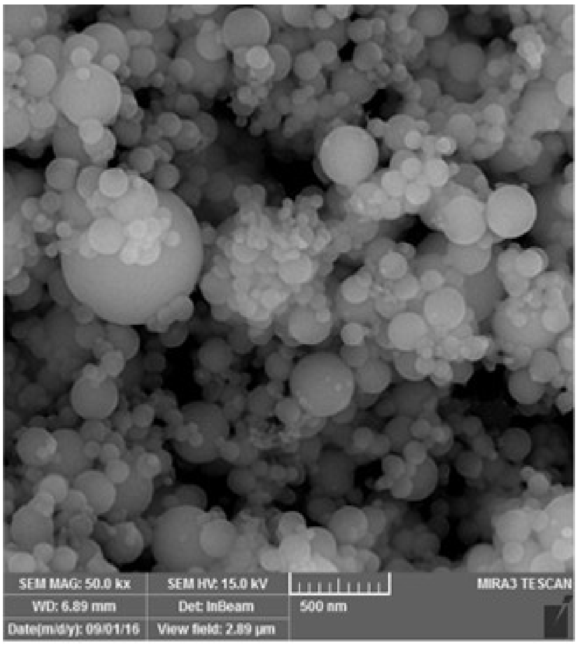

Figure 1: FESEM image of silica fume.

2.2 Method of Adsorption

Batch adsorption experiments are carried out to evaluate the adsorption performance of the adsorbent. A stock solution of 1000 ppm from dye have been used through the adsorption test. The stock solution was diluted with distilled water to give the appropriate concentration of the working solutions. Batch adsorption experiments were performed by contacting 0.1-0.5 g of silica fume samples with 100 mL of an aqueous solution of DO26 of the desired concentration and pH. The residual DO26 after adsorption was measured with a UV/visible spectrometer (UV2100, Unique, USA) at a λ_{max} corresponding to the maximum absorption for DO26 (λ_{max}=495 nm); the percent removal of DO26 as the main goal of the experiments is obtained from the following equation:

$$\%R=\frac{C_o - C_e}{C_o}\times 100 \quad \text{(Eq. 1)}$$

Where R is the percent removal, C_0 is the initial concentration of dye in the aqueous solution (mg/L), and C_e is the equilibrium concentration (mg/L).

The adsorption capacity of q (mg/g), as the main goal of the experiments, is obtained from the following equation:

$$q=\frac{C_o - C_f}{M}\times V \quad \text{(Eq. 2)}$$

Where q is the adsorption capacity at time t (mg/g), C_0 is the initial concentration of dye in the aqueous solution (mg/L), C_f is the concentration of dye after the adsorption at time t (mg/L), V is the volume of the aqueous solution (L), and M is the amount of adsorbent (g).

2.3 CCD method

Experiments are used to study process and system performance. A process or system is a combination of methods, operations, people, and other resources that transform input into output with one or more response variables by changing parameters. Checking the parameters and their effect on the system is done with one-variable, two-variable, and multi-variable methods. The univariate method, by changing one parameter and considering the other parameters is time-consuming and expensive. To solve these problems, experimental design is performed (Dbik et al., 2022). Experimental design causes process evaluation, process efficiency improvement, design selection in such a way that the product or output works well in different conditions, determination of key process parameters that have the greatest impact on process output (Montgomery, 2017).

There are various methods for experimental design, such as sk factorial designs, fractional factorial designs, block designs, response surface method (RSM), etc. (Montgomery, 2017).

RSM method is a set of applied statistical-mathematical methods for analyzing and modeling problems with different parameters to optimize the answer. The following equation shows the linear relationship between response and independent variables (Dargahi et al., 2021):

$$y=b_o+\sum b_i x_i \quad \text{(Eq. 3)}$$

This model is obtained in 2^k factorial design or 2^{k-p} fractional factorial design. It describes the linear relationship between the upper and lower levels and the behavior related to these two levels. If the relationship is not linear, the investigations require at least three levels, and polynomials with a higher power, such as quadratic polynomials, which are defined as follows, should be used (Geyikçi, Kılıç, Çoruh, & Elevli, 2012):

$$y=b_o+\sum b_i x_i+\sum b_{ii} x_i^2+\sum b_{ij} x_i x_j \quad \text{(Eq. 4)}$$

b_o is the linear constant, b_i is the coefficient of the linear part, b_{ii} is the coefficient of the quadratic part, and b_{ij} is the interaction coefficient.

CCD method includes 2^k full factor or fractional factor, which is coded as ±1 in the linear model, with 2k fractional tests and intersection of the axial or star fraction with the axial distance α, which gives us information about the quadratic model, and n_c tests in the central points, then the total number of tests in the CCD method is calculated (Geyikçi, Kılıç, Çoruh, & Elevli, 2012):

$$N=2^k+2k+n_c \quad \text{(Eq. 5)}$$

One of the most important parts of statistical research is choosing the appropriate statistical analysis method, which usually determines the type of statistical tests from the characteristics of the sample and the type of analysis required by the person doing the experiment. Statistical analysis can be done with parameters such as mean and variance. Many statistical tests are parametric, such as T-test and analysis of variance (Aziz et al., 2022).

3. RESULTS AND DISCUSSION

3.1 Impact of pH on Adsorption

The impact of pH on the adsorption of DO26 for 50 ppm DO26 solution by silica fume was investigated in the pH range of 2-11. The pH levels were adjusted using dilute solutions of HCl and NaOH. The experiment was carried out for 60 minutes with a stirring speed of 300 rpm. After adsorption, the solution was centrifuged, and the adsorption value was measured using a spectrophotometer. Figure 2a presents the effect of pH on the adsorption capacity of DO26 using silica fume. When the initial pH value of the DO26 solution was increased from 2 to 11, the adsorption capacity decreased from 10.48 to 2.891 mg/g. Due to the anionic nature of DO26, an increase in the electrostatic attraction force between the dye and adsorbent was observed at lower pH values and increased adsorption capacity. The maximum adsorption capacity of 10.48 mg/g was observed at pH 2.

3.2 Impact of Contact Time on Adsorption

The relation between adsorption capacity of DO26 and contact time was investigated for 20 to 90 minutes. Figure 2b shows the effect of contact time on the adsorption capacity of DO26 using silica fume at pH 2. According to the results, an increase in contact time led to an increase in the amount adsorbed until equilibrium was reached. In this study, equilibrium was reached after 40 minutes of adsorption.

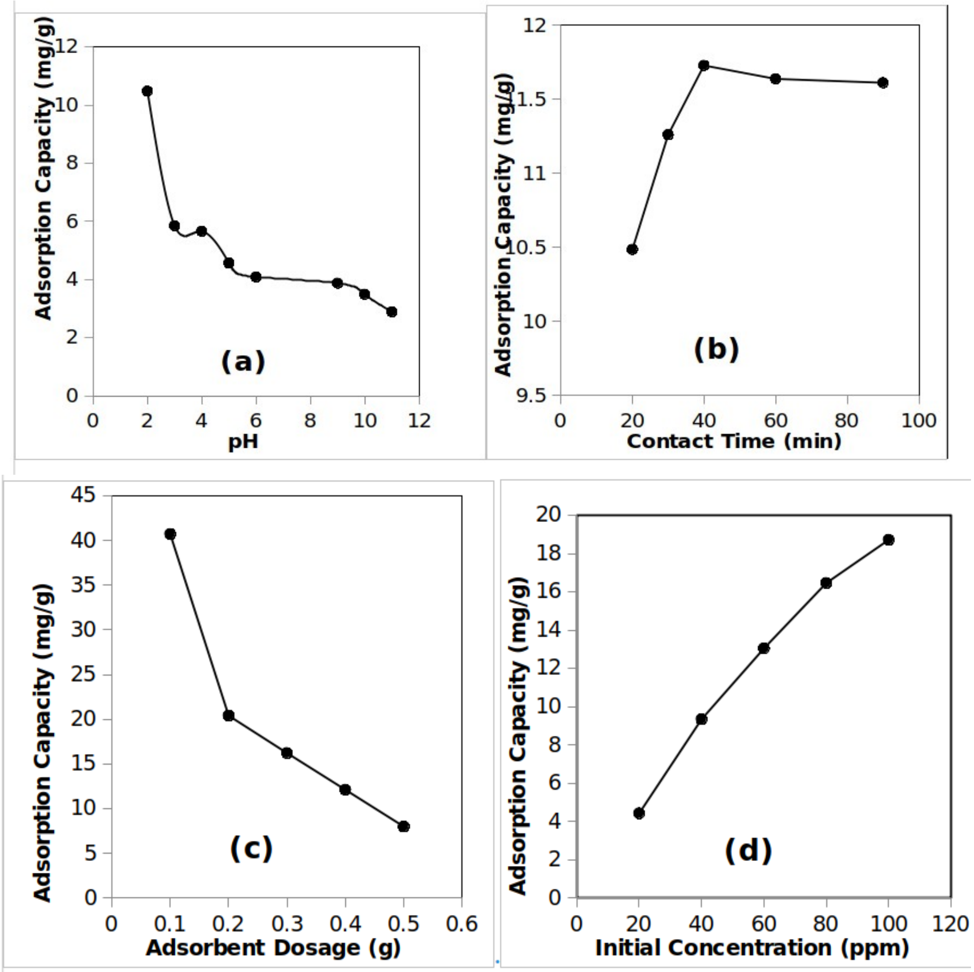

Figure 2: Effect of **a)** pH, **b)** contact time, **c)** the amount of adsorbent, and **d)** Initial Concentration on DO26 adsorption using silica fume.

3.3 Impact of the amount of adsorbent

Figure 2c shows the impact of the amount of adsorbent on the adsorption capacity of DO26 using silica fume at pH 2. The adsorption capacity of DO26 decreased from 40.7185 to 8.0045 mg/g as the amount of silica fume increased from 0.1- 0.5 g. An increase in the amount of adsorbent reduces the number of active adsorption sites, leading to a decrease in adsorption capacity and affecting the overall process.

3.4 Impact of Initial Concentration of the Solution on Adsorption

Figure 2d shows the effect of the initial DO26 concentration on the adsorption capacity using silica fume. These data have been obtained over the initial concentration range of 20 to 100 ppm for DO26 at pH 2. In this study, the adsorption capacity of DO26 increased as the initial DO26 concentration increased from 20- 100 ppm. According to the result, silica fume has an excellent potential for removal of DO26 from wastewater.

3.5 Kinetic study

To understand the rate and adsorption mechanism involved in the removal of DO26 by the silica fume, the experimental kinetic data were analyzed through the conventional kinetic models including pseudo-first order, pseudo-second order, and Elovich equations. The linear form of the equation corresponding to each kinetic model and the relative parameters that were calculated are summarized in Table (2).

The results demonstrate that the sorption kinetics can be accurately described by the pseudo-second order model. The high regression correlation coefficients (R^2 = 0.9992) and the close agreement between experimental and theoretical adsorption capacity (qe) values confirm that chemisorption is the rate-controlling step throughout the entire adsorption process.

Table 2: Summary of the kinetics models for adsorption of DO26 on silica fume.

Model	Equation	Parameters	Values of parameters
First-order	$\mathrm{Ln}\left(q_e - q_t\right) = \mathrm{Ln}\, q_e - K_1$	K_1 (L/min) q_e (mg/g) R^2	0.0182 0.9977 0.3815
Second-order	$\mathrm{Ln}\left(q_e - q_t\right) = \mathrm{Ln}\, q_e - K_1$	K_2 (g/mg min) q_e (mg/g) R^2	0.0487 11.9110 0.9992
Elovich	$\mathrm{Ln}\left(q_e - q_t\right) = \mathrm{Ln}\, q_e - K_1$	β α R^2	1.4643 2.7090×10^5 0.6427

3.6 CCD Design and Experimental Response

The effect of absorption parameters pH, adsorbent amount, contact time, initial dye concentration, optimal temperature, and absorption rate were investigated. Then, design of experiment was carried out in the optimal range to investigate the interaction effects of the parameters of the absorption process at three levels. In this study, Design Expert software version of 7 was used. Parameter of pH checked at three levels of 4, 3, and 2, the absorption amount was checked at the levels of 0.4, 0.3, and 0.2, the time levels were 60, 45, and 30, and the concentration checked at the three levels of 60, 40, and 20. CCD design matrix and experimental response values are presented in Table (3).

According to the ANOVA results for the quadratic model, effect of pH, amount of adsorbent, concentration and interaction between pH and amount of adsorbent, pH and concentration, amount of adsorbent and time, amount of adsorbent and concentration, time and concentration and the double effect of the adsorbent parameters are important and effective for designing model. ANOVA of the regression model is exhibited in Table 4 for DO26. The Model F-value of 135.65 implies the model is significant. There is only a 0.01% chance that an F-value this large could occur due to noise. P-values less than 0.0500 indicate model terms are significant. In this case, A, C, D, AB, AC, AD, BC, CD, A^2, B^2, C^2, D^2 are significant model terms. Values above 0.1000 suggest that the model terms are not significant.

In all experiments, temperature and stirring speed were kept constant. The software examines different models to predict the removal percentage and suggests a model with significant values. In the experimental design for DO26 in the present study, the model proposed by the software is a second-order model. A summary of polynomial models is presented in Table (5).

Table 3. CCD design matrix and experimental response values.

Run	Factor 1 A: pH	Factor 2 B: m (g)	Factor 3 C: Time (min)	Factor 4 Concentration (ppm)	Response $R1_{experimental}$	Response $R1_{predicted}$
1	4.00	0.40	60.00	60.00	19.9714	19.9315
2	4.00	0.30	45.00	40.00	16.3941	19.9393
3	4.00	0.20	60.00	60.00	23.008	20.3868
4	4.00	0.20	60.00	20.00	36.4599	35.9982
5	2.00	0.40	60.00	20.00	80	77.5424
6	3.00	0.40	45.00	40.00	52.3493	52.3493
7	3.00	0.30	45.00	40.00	33.1254	30.4402
8	3.00	0.30	45.00	40.00	26.5876	30.4402
9	3.00	0.30	60.00	40.00	31.1372	30.6154
10	2.00	0.40	30.00	60.00	79.0333	78.5115
11	2.00	0.40	30.00	20.00	43.6679	47.2111
12	3.00	0.30	45.00	40.00	30.005	30.4402
13	2.00	0.20	30.00	20.00	50.007	49.0634
14	3.00	0.30	45.00	40.00	27.9823	30.4402
15	2.00	0.20	30.00	60.00	75.2386	74.4880
16	3.00	0.30	45.00	40.00	31.7921	30.4402
17	3.00	0.30	45.00	60.00	27.0744	26.2156
18	3.00	0.20	45.00	40.00	48.6275	51.1883
19	3.00	0.30	30.00	40.00	18.9089	19.6766
20	4.00	0.40	30.00	60.00	44.1021	44.0073
21	3.00	0.30	45.00	40.00	33.8864	30.4402
22	4.00	0.40	60.00	20.00	27.9946	29.6672
23	4.00	0.40	30.00	20.00	24	21.9084
24	2.00	0.40	60.00	60.00	74.7034	77.0081
25	4.00	0.20	30.00	60.00	27.3663	28.8405
26	2.00	0.20	60.00	20.00	94	95.0168
27	2.00	0.20	60.00	60.00	87.4986	88.6068
28	2.00	0.30	45.00	40.00	70	66.7007
29	3.00	0.30	45.00	20.00	17.2663	18.3711
30	4.00	0.20	30.00	20.00	14	12.6173

The final quadratic model with R^2=0.9922 was obtained as follows:
$R1=+181.68-87.49A-1211.82B+5/45C+3.148D+27.86AB-0.38AC-0.12AD-2.60+0.73BD-0.026CD+12.88A^2+2017.11B^2-0.02C^2-0.02D^2$

A: pH
B: adsorbent
C: time
D: concentration
And the binary combination of parameters is obtained by multiplying the symbols.

Table 4. ANOVA for response surface quadratic model for DO26 removed by silica fume.

Source	Sum of Squares	df	Mean Square	F-value	p-value	
Model	16005.59	14	1143.26	135.65	< 0.0001	Significant
A-PH	9839.82	1	9839.82	1167.48	< 0.0001	
B-m	5.99	1	5.99	0.7107	0.4124	
C-Time	538.46	1	538.46	63.89	< 0.0001	
D-concentration	276.91	1	276.91	32.86	< 0.0001	
AB	124.17	1	124.17	14.73	0.0016	
AC	509.51	1	509.51	60.45	< 0.0001	
AD	84.67	1	84.67	10.05	0.0063	
BC	244.05	1	244.05	28.96	< 0.0001	
BD	34.52	1	34.52	4.10	0.0612	
CD	1013.44	1	1013.44	120.24	< 0.0001	
A^2	429.81	1	429.81	51.00	< 0.0001	
B^2	1054.19	1	1054.19	125.08	< 0.0001	
C^2	72.62	1	72.62	8.62	0.0102	
D^2	171.96	1	171.96	20.40	0.0004	
Residual	126.42	15	8.43			
Lack of Fit	84.53	10	8.45	1.01	0.5306	not significant
Pure Error	41.90	5	8.38			
Cor Total	16132.02	29				

Table 5: Summary of the models for adsorption of DO26 on silica fume.

Source	Sum of Squares	df	Mean Squares	F Value	p-value Prob > F	
Mean vs Total	53441.60	1	53441.60			
Linear vs Mean	10661.35	4	2665.34	12.18	< 0.0001	
2FI vs Linear	2010.45	6	335.08	1.84	0.1447	
Quadratic vs 2FI	3334.13	4	833.53	98.88	< 0.0001	Suggested
Cubic vs Quadratic	80.70	8	10.09	1.54	0.2903	Aliased
Residual	45.75	7	6.54			
Total	69573.99	30	2319.13			

In Figure 3, the response surface diagrams are presented to investigate the effective parameters for absorption of DO26 on silica fume. The highest percentage of removal was predicated 95.26% by the software (pH=2.01, adsorbent amount=0.2 g, time=55.15 minutes, and concentration=44 ppm).

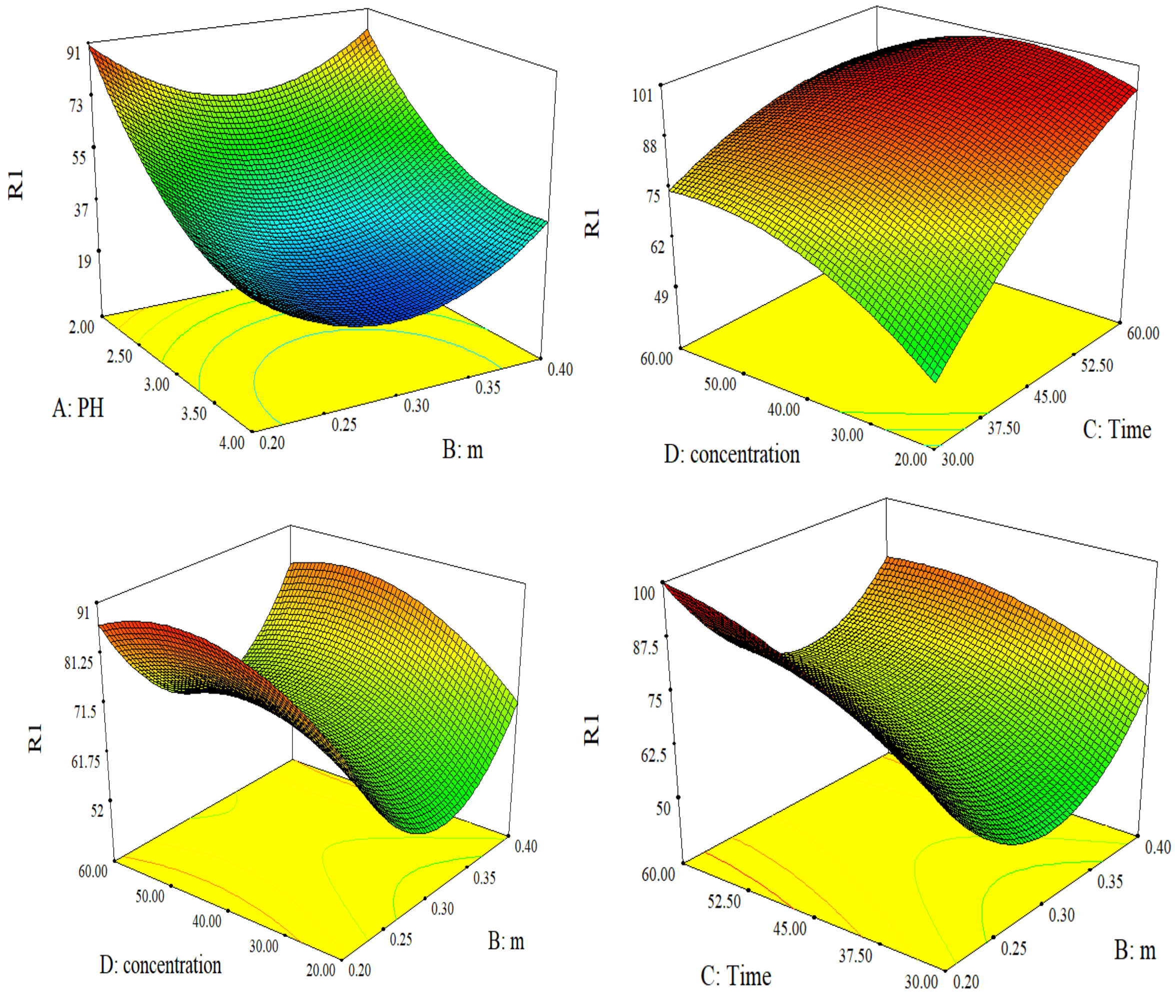

Figure 3: 3D surface plot of DO26 adsorption on silica fume.

Table 6. Summary of kinetics and RSM optimization of the present study and previous studies.

Adsorbent	Dye	Kinetic model	Optimum conditions A=pH B=adsorbent C=time D=concentration	%$R_{predicated}$	Reference
Silica fume	DO26	pseudo-second-order	A=2.01 B=0.2 g c=55.15 min D=44 ppm	95.26%	Present study
Carbon Nano tube doped ZnO/ Fe_2O_3	DO26	pseudo-second-order	A=5 C=3.8 hours	70.6%	(Tariq et al., 2022)
Cerium- doped mesoporous ZnO	DR81	-	A=3 B=0.02 g C=19.68 min D=40 ppm	94.41%	(Bazgir et al., 2019)
Kola nut shell activated carbon	orange G	-	A=6.0 B=0.30 g C=60 min D=100 mg/l	93.93%	(Chinonye et al., 2018)

4. CONCLUSION

In this study, adsorption of DO26 azo dye on silica fume in a batch system was investigated. Design of the experiment was carried out with CCD method to model and influence the interaction effects of the parameters. According to the ANOVA results for the quadratic model, effect of pH, amount of adsorbent, concentration and interaction between pH and amount of adsorbent, pH and concentration, amount of adsorbent and time, amount of adsorbent and concentration, time and concentration and the double effect of the adsorbent parameters are important and effective. The optimum conditions for maximum removal of DO26 (95.26%) were obtained to be at pH 2.01, contact time 55.15 minutes, adsorbent amount=0.2 g, and initial concentration 44 ppm. The experimental kinetic data were analyzed through the conventional kinetic models, and the results demonstrate that the sorption kinetics can be accurately described by the pseudo-second order model. The literature on the absorption of azo dyes was reviewed, and the findings of this study were compared to previous research in terms of kinetics and RSM outcomes. The summarized results, presented in Table 6, indicate that silica fume outperformed other adsorbents in terms of optimal removal percentage of the dye. Also, according to the FESEM image, silica fume has a spherical and porous structure; Therefore, silica fume as a cheap adsorbent can remove dye pollutants from water.

5. REFERENCES

Ahmed, S. A., Gaber, A. A. A., & Rahim, A. M. A. (2017). Application of silica fume as a new SP-extractor for trace determination of Zn (II) and Cd (II) in pharmaceutical and environmental samples by square-wave anodic stripping voltammetry. Applied Water Science, 7(2), 677-688.

Aşçı, Y. (2013). Decolorization of Direct Orange 26 by heterogeneous Fenton oxidation. Desalination and Water Treatment, 51(40-42), 7612-7620.

Aziz, K., Aziz, F., Mamouni, R., Aziz, L., Anfar, Z., Azrrar, A., . . . Laknifli, A. (2022). High thiabendazole fungicide uptake using Cellana tramoserica shells modified by copper: Characterization, adsorption mechanism, and optimization using CCD-RSM approach. Environmental Science and Pollution Research, 29(57), 86020-86035.

Bazgir, A., Khorshidi, A., Kamani, H., Ashrafi, S. D., & Naghipour, D. (2019). Modeling of azo dyes adsorption on magnetic NiFe 2 O 4/RGO nanocomposite using response surface methodology. Journal of Environmental Health Science and Engineering, 17, 931-947.

Chinonye, O.A., Oluchukwu, A.C., & Elijah, O.C. (2018), Statistical analysis for orange G adsorption using kola nut shell activated carbon. Journal of the Chinese Advanced Materials Society, 6(4), 605-619.

Dargahi, A., Samarghandi, M. R., Shabanloo, A., Mahmoudi, M. M., & Nasab, H. Z. (2021). Statistical modeling of phenolic compounds adsorption onto low-cost adsorbent prepared from aloe vera leaves wastes using CCD-RSM optimization: effect of parameters, isotherm, and kinetic studies. Biomass Conversion and Biorefinery, 1-15.

Dbik, A., El Messaoudi, N., Bentahar, S., El Khomri, M., Lacherai, A., & Faska, N. (2022). Optimization of Methylene Blue Adsorption on Agricultural Solid Waste Using Box–Behnken Design (BBD) Combined with Response Surface Methodology (RSM) Modeling. Biointerface Research in Applied Chemistry, 12(4), 4567-4583.

Genc, A., & Oguz, A. (2010). Sorption of acid dyes from aqueous solution by using non-ground ash and slag. Desalination, 264(1-2), 78-83.

Geyikçi, F., Kılıç, E., Çoruh, S., & Elevli, S. (2012). Modelling of lead adsorption from industrial sludge leachate on red mud by using RSM and ANN. Chemical Engineering Journal, 183, 53-59.

Ghaedi, M., Hajati, S., Zaree, M., Shajaripour, Y., Asfaram, A., & Purkait, M. (2015). Removal of methyl orange by multiwall carbon nanotube accelerated by ultrasound devise: Optimized experimental design. Advanced Powder Technology, 26(4), 1087-1093.

Kalkan, E., Nadaroglu, H., & Celebi, N. (2014). Use of Silica Fume as Low-Cost Absorbent Material for Nickel Removal from Aqueous Solutions. Asian Journal of Chemistry, 26(18).

Kannaujiya, M. C., Gupta, G. K., Mandal, T., & Mondal, M. K. (2022). Adsorption of Acid Yellow 2GL dye from simulated water using brinjal waste. Biomass Conversion and Biorefinery, 1-14.

Li, X., Han, C., Zhu, W., Ma, W., Luo, Y., Zhou, Y., . . . Wei, K. (2014). Cr (VI) removal from aqueous by adsorption on amine-functionalized mesoporous silica prepared from silica fume. Journal of Chemistry, ID 765856, 1-10.

Montgomery, D. C. (2017). Design and analysis of experiments: John wiley & sons.

Nadaroglu, H., & Kalkan, E. (2014). Removal of copper from aqueous solution using activated silica fume with/without apocarbonic anhydrase.

Safa, Y., & Bhatti, H. N. (2011). Kinetic and thermodynamic modeling for the removal of Direct Red-31 and Direct Orange-26 dyes from aqueous solutions by rice husk. Desalination, 272(1-3), 313-322.

Sohrabi, M. R., Moghri, M., Masoumi, H. R. F., Amiri, S., & Moosavi, N. (2016). Optimization of Reactive Blue 21 removal by Nanoscale Zero-Valent Iron using response surface methodology. Arabian journal of chemistry, 9(4), 518-525.

Tariq, W., Arslan, C., Naqvi, S. A., Abdullah, M., Nasir, A., Gillani, S. H., . . . Yamin, M. (2022). Photocatalytic Removal of Azo Dyes Using a CNT Doped ZnO/Fe₂O₃ Catalyst. Polish Journal of Environmental Studies, 31(5), 4279-4289. doi:10.15244/pjoes/131805

Tomczak, E., & Tosik, P. (2014). Sorption equilibrium of azo dyes Direct Orange 26 and Reactive Blue 81 onto a cheap plant sorbent. Ecological Chemistry and Engineering.

Wang, Y., & Chu, W. (2011). Adsorption and removal of a xanthene dye from aqueous solution using two solid wastes as adsorbents. Industrial & engineering chemistry research, 50(14), 8734-8741.

Yan, L.-g., Qin, L.-l., Yu, H.-q., Li, S., Shan, R.-r., & Du, B. (2015). Adsorption of acid dyes from aqueous solution by CTMAB modified bentonite: kinetic and isotherm modeling. Journal of Molecular Liquids, 211, 1074-1081.

Zhang, D., Ma, Y., Feng, H., Wang, Y., & Hao, Y. (2012). Preparation and characterization of the carbon–Microsilica composite sorbent. Advanced Powder Technology, 23(2), 215-219.

Zhu, X., Zhang, Z., & Yan, G. (2016). Methylene blue adsorption by novel magnetic chitosan nanoadsorbent. Journal of Water and Environment Technology, 14(2), 96-105.